In vivo mouse studies with bioluminescence tomography

Ge Wang[1], Wenxiang Cong[1], Kumar Durairaj[1], Xin Qian[1], Haiou Shen[1], Patrick Sinn[2], Eric Hoffman[1], Geoffrey McLennan[2], and Michael Henry[3]

[1]Bioluminescence Tomography Laboratory, Department of Radiology
[2]Department of Internal Medicine
[3]Department of Physiology & Biophysics
University of Iowa, 200 Hawkins Drive, IA 52242, USA
ge-wang@ieee.org, wenxiang-cong@uiowa.edu

Bioluminescence tomography (BLT) is a new molecular imaging mode, which is being actively developed to reveal molecular and cellular signatures as labeled by bioluminescent probes in a living small animal. This technology can help diagnose diseases, evaluate therapies, and facilitate drug development with mouse models. In this paper, we describe *in vivo* mouse experiments with BLT, and propose the reconstruction procedure of bioluminescent sources from optical data measured on the body surface of the mouse using a modality fusion approach. The results show the feasibility of our methodology for localization and quantification of the bioluminescent activities *in vivo*.

OCIS codes: (170.6960) Tomography; (170.3010) Image reconstruction techniques; (170.3660) Light propagation in tissues.

References and links

1. V. Ntziachristos, J. Ripoll, L. V. Wang, R. Weissleder, "Looking and listening to light: the evolution of whole-body photonic imaging," Nat. Biotechnol. **23**, 313-320 (2005).
2. C. Contag and M. H. Bachmann, "Advances in Bioluminescence imaging of gene expression," Annu. Rev. Biomed. Eng. 4, 235-260 (2002).
3. W. Rice, M. D. Cable, and M. B. Nelson, "*In vivo* imaging of light-emitting probes," J. Biomed. Opt. **6**, 432-440 (2001).
4. G. Wang, E. A. Hoffman, and G. McLennan, Systems and methods for bioluminescent computed tomographic reconstruction. Patent disclosure filled in July 2002; US provisional patent application filled in March 2003; US patent application filed in March 2004.
5. G. Wang, E. A. Hoffman, G. McLennan, L. V. Wang, M. Suter, and J. Meinel, "Development of the first bioluminescent CT scanner," Radiology **229**, 566 (2003).
6. G. Wang, Y. Li, and M. Jiang, "Uniqueness theorems in bioluminescence tomography," Med. Phys. **31**, 2289-2299 (2004).
7. W. Cong, D. Kumar, Y. Liu, A. Cong, and G. Wang, "A practical method to determine the light source distribution in bioluminescent imaging," in Developments in X-Ray Tomography IV; U. Bonse, ed., Proc. SPIE **5535**, 679-686 (2004).
8. W. Cong, G. Wang, D. Kumar, Y. Liu, M. Jiang, L. Wang, E. Hoffman, G. McLennan, P. McCray, J. Zabner, and A. Cong, "Practical reconstruction method for bioluminescence tomography," Opt. Express **13**, 6756-6771 (2005).
9. X. Gu, Q. Zhang, L. Larcom, and H. Jiang, "Three-dimensional bioluminescence tomography with model-based reconstruction," Opt. Express **12**, 3996-4000 (2004).
10. W. Cong and G. Wang, "Boundary integral method for bioluminescence tomography," J. Biomed. Opt. **11**, 020503 (2006).
11. M. Jiang, and G. Wang, "Image reconstruction for bioluminescence tomography," in Developments in X-Ray Tomography IV, U. Bonse, ed., Proc. SPIE **5535**, 335-351 (2004).
12. N.V. Slavine, M.A. Lewis, E. Richer, P.P. Antich, "Iterative reconstruction method for light emitting sources based on the diffusion equation," Med. Phys. **33**, 61-68 (2006).
13. G. Alexandrakis, F. R. Rannou, and A. F. Chatziioannou, "Tomographic bioluminescence imaging by use of a combined optical-PET (OPET) system: a computer simulation feasibility study," Phys. Med. Biol. **50**, 4225–4241 (2005).

#70324 - $15.00 USD Received 26 April 2006; revised 27 July 2006; accepted 27 July 2006

14. A. J. Chaudhari, F. Darvas, J. R. Bading, R. A. Moats, P. S. Conti, D. J. Smith, S. R. Cherry and R. M. Leahy, "Hyperspectral and multispectral bioluminescence optical tomography for small animal imaging," Phys. Med. Biol. **50**, 5421–5441 (2005).
15. A. X. Cong and G. Wang, "Multi-spectral bioluminescence tomography: Methodology and simulation," International Journal of Biomedical Imaging **2006**, ID57614, 1-7 (2006).
16. H. Dehghani, S. C. Davis, S. Jiang, B. W. Pogue, and K. D. Paulsen, "Spectrally resolved bioluminescence optical tomography," Opt. Lett. **31**, 365-367 (2006).
17. M. Schweiger, S. R. Arridge, M. Hiraoka, and D. T. Delpy, "The finite element method for the propagation of light in scattering media: Boundary and source conditions," Med. Phys. **22**, 1779- 1792 (1995).
18. A. J. Welch and M. J. C. Van Gemert, Optical and Thermal response of laser-irradiated tissue (Plenum Press, New York, 1995).
19. J. M. Drake, C. L. Gabriel, and M. D. Henry, "Assessing tumor growth and distribution in a model of prostrate cancer metastasis using bioluminescence imaging," Clin. Exp. Metastasis PMID: 16703413, [Epub ahead of print] (2006).
20. A. Rehemtulla, L. D. Stegman, S. J. Cardozo, S. Gupta, D. E. Hall, C. H. Contag, and B. D. Ross, "Rapid and quantitative assessment of cancer treatment response using *in vivo* bioluminescence imaging," Neoplasia **2**, 491-495 (2000).

1. Introduction

Bioluminescent signals reveal molecular and cellular activities *in vivo*. Bioluminescent imaging (BLI) can be applied to study many physiological and pathological processes in various small animal models. Hence, it becomes an increasingly important tool for biomedical researchers to diagnose diseases, evaluate therapies, and facilitate drug development with mouse models [1-2]. BLI is traditionally in a planar mode largely as a qualitative tool [3]. With the introduction of bioluminescence tomography (BLT), a bioluminescent source distribution inside a living small animal can be localized and quantified in 3D [4-6]. The significance of this advancement can be likened to the development of x-ray CT based on radiography. In comparison with other optical biomedical imaging techniques, BLT is unique in terms of its sensitivity and specificity.

The bioluminescent photons cover a red region of the spectrum with a deep penetration depth [2]. Hence, a significant number of the photons can escape the attenuating environment, and be detected using a highly sensitive charge-coupled device (CCD) camera. Photon migration through the biological tissue is subject to both scattering and absorption. In the biological tissue the photon scattering dominants over photon absorption. Furthermore, since the biological tissue does not emit photons while the tissue is not excited by external light, the background noise in bioluminescent imaging is very low, which results in an excellent signal-to-noise ratio.

The transmission of bioluminescent photon depends on not only the optical properties of tissue but also on the geometrical model of the mouse. The anatomic structure information of the small animal can be imaged by X-ray CT and MRI techniques, and the geometrical shape of major organ regions is established by 3D computer graphic techniques. Every organ region can be associated with tissue optical parameters which are determined by optical tomographic approach. Based upon the geometrical and optical properties model, the BLT can be reduced to an inverse source problem of differential equation. The BLT principles and solution uniqueness were theoretically studied [5, 6]. Some numerical BLT algorithms were already reported, including the finite element and boundary element based BLT algorithms [7-10], EM reconstruction technique for BLT [11, 12], BLT in combination with PET (OPET) [13], multispectral BLT [14-16]. In this paper, we describe *in vivo* mouse experiments with BLT, and reconstruct bioluminescent sources from optical data measured on the body surface of the mouse using a modality fusion approach. We emphasize that our report is the first *in vivo* BLT study using the deformable atlas based meshing approach to compensate for the anatomical heterogeneity.

2. System design and methodology

We have developed a BLT system for mouse molecular imaging, as shown in Fig. 1. The BLT system uses a CCD camera (Princeton Instruments VA 1300B, Roper Scientific, Trenton, NJ)

#70324 - $15.00 USD Received 26 April 2006; revised 27 July 2006; accepted 27 July 2006

to collect bioluminescent signals around a mouse. A stage is vertically rotated under computer control to acquire bioluminescent views around the mouse. A stage is vertically rotated under computer control for acquisition of bioluminescent views around the mouse. A Nikon Normal Macro 55mm f/2.8 Micro Nikkor Manual Focus Lens was used in the BLT system. The lens has the minimum focus distance 10"(25cm). During the imaging experiment, the aperture was fully open while the mouse was kept at the minimum focus distance. The distance between the lens and the mouse skin was adjusted and measured by a manually controlled linear transport for the best image clarity. A holder maintains the mouse in a vertical position, and clamps onto the rotation stage. Marks are placed on the mouse skin for registration with a CT image volume of the same mouse. To perform the bioluminescence imaging experiment in a totally dark environment, a light-tight enclosure, built out of 1/2" plywood lined with aluminums and black felt, has an entry hatch to accommodate the wires and minimize light leaking. The front side of the box is removable (not in this photograph) for manipulation of the mouse. The camera generates 1340 by 1300 16-bit images of 20μm by 20μm pixels. Typically, at each orientation, two images are obtained with light on and off for exposure time 0.1second and 5-25minutes, respectively. The former image indicates the mouse body surface. The latter image represents the bioluminescent view from the corresponding orientation relative to the mouse body.

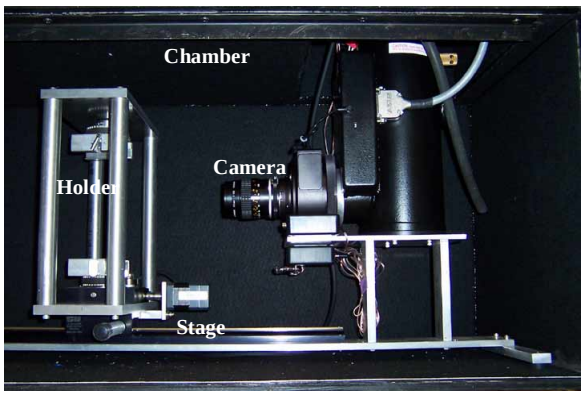

Fig. 1. Our first BLT system consisting of a mouse stage, a CCD camera, a mouse holder and so on.

Several days before our experiments using the BLT system, light-emitting luciferase probes are implanted into a mouse. At the beginning of the bioluminescence imaging experiment, the luciferase substrate luciferin is injected into the mouse. Then, a biochemical reaction generates bioluminescent photons in the biological tissue. The photon fluence rate is detected on the side surface of the mouse using the sensitive CCD system. The bioluminescent photon scattering predominates over absorption in the mouse tissue. Hence, the propagation of these photons can be modeled as a diffusive process. Because the internal bioluminescent light is continuously on during the measurement, BLT operates only in the CW mode. In this case, the photon propagation in the biological tissue can be well described by the steady-state diffusion equation and the Robin boundary condition [17, 18],

$$\begin{cases} -\nabla\cdot\left(D(\mathbf{r})\nabla\Phi(\mathbf{r})\right)+\mu_a(\mathbf{r})\Phi(\mathbf{r})=S(\mathbf{r}) \quad (\mathbf{r}\in\Omega) \\ \Phi(\mathbf{r})+2A(\mathbf{r})D(\mathbf{r})\left(\mathbf{v}(\mathbf{r})\cdot\nabla\Phi(\mathbf{r})\right)=0 \quad (\mathbf{r}\in\partial\Omega) \end{cases} \tag{1}$$

where $\Phi(\mathbf{r})$ represents the photon fluence rate [Watts/mm^2] at location $\mathbf{r}$, $S(\mathbf{r})$ the density of the bioluminescent source distribution [Watts/mm^3], $\mu_a(\mathbf{r})$ the absorption coefficient

#70324 - $15.00 USD Received 26 April 2006; revised 27 July 2006; accepted 27 July 2006

[mm^{-1}], $\mu_s'(\mathbf{r})$ the reduced scattering coefficient [mm^{-1}], $D(\mathbf{r}) = \left(3\left(\mu_a(\mathbf{r}) + \mu_s'(\mathbf{r})\right)\right)^{-1}$ the diffusion coefficient, Ω the support for the mouse body, $\partial\Omega$ the body surface of the mouse, and $A(\mathbf{r})$ the mismatch coefficient due to different refractive indices across $\partial\Omega$. With an adequate exposure time, a significant amount of bioluminescent photons can reach the body surface of the mouse and be detected with a highly sensitive CCD camera. The measured quantity is the photon current on the body surface of the mouse:

$$\tilde{\Phi}(\mathbf{r}) = -D(\mathbf{r})\left(\mathbf{v}\cdot\nabla\Phi(\mathbf{r})\right) \quad (\mathbf{r}\in\partial\Omega), \tag{2}$$

where $\mathbf{v}$ denotes the unit outer normal to $\partial\Omega$. Based on Eqs. (1) - (2), a linear system linking a bioluminescent source distribution and the boundary measurement data can be obtained as [7, 8, 10]

$$\mathbf{A}\,\mathbf{S} = \tilde{\mathbf{\Phi}}. \tag{3}$$

where $\mathbf{S} = \{S_1, S_2, \cdots, S_M\}$ represents the bioluminescence source distribution, $\mathbf{A} = \{\mathbf{a}^1, \mathbf{a}^2, \cdots, \mathbf{a}^M\}$ a weighting matrix consisting of N-dimensional column vectors $\mathbf{a}^k$ about source distribution $(k = 1, 2, \cdots, M)$, and $\tilde{\mathbf{\Phi}}$ an N-dimensional vector computed from the bioluminescent data measured on the body surface of the mouse. Clearly, $S_k\mathbf{a}^k$ is the contribution of the k-th source component S_k to $\tilde{\mathbf{\Phi}}$. Then, the BLT problem becomes to reconstruct S_i $(i = 1, 2, \cdots, M)$ from the data $\tilde{\mathbf{\Phi}}$ measured on the mouse body surface.

BLT is to reconstruct a 3D bioluminescent source distribution inside a living mouse based on the bioluminescent signal on the mouse body surface. These externally observable optical data are calculated from pixel values in the bioluminescence images taken by the CCD camera. These pixel values are strongly correlated. In general, the number of unknown variables of the underlying bioluminescence source distribution is much more than the number of independent measures at the surface nodes. Hence, BLT is a typical underdetermined problem [6], and strong prior knowledge must be incorporated into the reconstruction process to overcome the ill-posedness of the problem effectively. In this context, the permissible source region was used to reduce the number of unknown variables and thus enhance the stability of the BLT algorithm. In the bioluminescence imaging experiment, planar bioluminescent views were acquired by the CCD camera. In these views, high value clusters clearly indicated the permissible source region. Then, a relatively large region was specified as the initial permissible region, and iteratively refined as necessary. The reconstructed results were obtained in reference to the permissible source region. In this study, we utilized a threshold of 10% of the maximum reconstructed source density to decrease the permissible region for improved results. Mathematically, given a permissible source region Ω_S the BLT reconstruction is equivalent to the following optimization subject to regularization [8],

$$\min_{\substack{0\le S\le U \\ S\in\Omega_S}} \left\|\mathbf{A}\,\mathbf{S} - \tilde{\mathbf{\Phi}}\right\|_W^2 + \varepsilon\eta(S), \tag{4}$$

where η a stabilizing function, ε a regularization parameter, W a weighting matrix, and $\|V\|_W^2 = V^T W V$. U denotes the upper bound for the source density to be physically meaningful.

In fact, the photon number emitted from a cell can be easily estimated in a bioluminescence imaging experiment. Hence, the upper bound of the power emitted in an element was

#70324 - $15.00 USD Received 26 April 2006; revised 27 July 2006; accepted 27 July 2006

approximated as the product of the number of cells in a finite element volume and the number of photons emitted from a cell.

3. Mouse experiments

We successfully performed *in vivo* mouse studies using BLT. Two representative cases are described as follows. In the first luminescent imaging experiment, a mouse was anesthetized with i.p. injection of 2.5% avertin 100μl/10g body weight. A luminescent light stick (Glowproducts, Victoria, Canada) at an emission wavelength range between ~650nm and ~700nm was selected as the testing source, which is close to that of the red spectral region of the luciferase [8]. The stick consists of a glass vial containing one chemical solution and a larger plastic vial containing another solution with the former being embedded in the latter. By bending the plastic vial, the glass vial can be broken to mix the two solutions into luminescent liquid and generate luminescent photons. One end tip of a catheter of 50mm length and 0.58mm diameter was filled with luminescent liquid to a 2mm height. Then, the catheter was inserted in the trachea through a tracheotomy incision. The luminescence liquid level inside the catheter occupied a small space from the tip of the tube, while the free volume at the tip was filled with the clay to avoid leakage of the fluid. Excepting for the distal liquid column surface, the tube was coated with black to avoid stray light. After placing the tube via the trachea to sit just within the origin of the right main bronchus, the outer exposed part of the tube was tied by a suture thread in the trachea just below the incision location. The mouse was immediately placed in the holder, and went through the BLT procedure to acquire luminescent data by CCD camera in four views around the mouse body. Four pseudo-color images were generated for the luminescent views, and superimposed on the corresponding photographs, as shown in Figs. 2(a)-2(d). Then, the mouse was frozen in liquid nitrogen to maintain upright organ orientations in the recumbent body posture, and scanned using a micro-CT scanner (SkyScan-1076, SkyScan, Aartselaar, Belgium), and the position of the catheter filled luminescent liquid can be identified from the CT slices, as shown in Fig. 4(b).

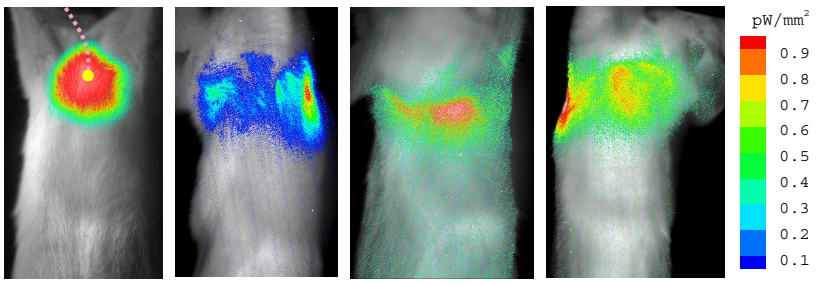

Fig. 2 Luminescent views (in pseudo color) of the side surface of the first mouse body taken by the CCD camera from four directions of 90 degrees apart. The luminescent views are superimposed on the corresponding mouse photographs. (a)-(d) Anterior-posterior, right lateral, posterior-anterior, left lateral views, respectively (the dotted pink line and the small yellow dot in (a) represent the path of the catheter and the luminescent liquid, respectively)

The semi-automatic deformation procedure is a practical segmentation method we developed in-house to combine computerized segmentation, optimal registration and expert intervention. In this procedure, an MRI mouse atlas from a NIH-supported project (http://www.mrpath.com/visiblemouse.html) was utilized to compensate for the sub-optimal contrast resolution of the CT scan. The CT slices of the mouse were segmented into major anatomical components, including lungs, a heart, a liver, a stomach, kidneys, *etc*. Using commercial software Amira 4.0 (Mercury Computer Systems, Inc. Chelmsford, MA), the mouse geometrical model was established for the mouse body as the region of interest consisting of 80670 tetrahedral elements and 14757 nodes, as shown in Fig. 3(a). Totally 2757 detectors were virtually located on the side surface of the mouse. The data in the four

#70324 - $15.00 USD Received 26 April 2006; revised 27 July 2006; accepted 27 July 2006

bioluminescent views were mapped onto the surface of the geometrical model, as shown in Fig. 3(b). Then, the detector readings were computed from the four CCD images in Fig. 2. The high value clusters in the bioluminescent views suggested a potential permissible source region, which was specified as $\Omega_s = \{(x,y,z) | -4.0<x<4.0,\ 0.0<y<4.0,\ 9.5<z<13.5\}$ to reduce the number of unknown variables. The appropriate absorption (μ_a) and transport scattering (μ_s') coefficients were assigned to each anatomical structure. These optical parameters were estimated based on the literature [13], as summarized in Table 1. In the aforementioned BLT reconstruction procedure, the stabilizing function was set to $\eta(\mathbf{r}) = \mathbf{r}^T\mathbf{r}$ with the regularization parameter ε being 1.0E-6. A modified Newton method and an active set strategy were performed subject to the upper bound of the source power intensity. Furthermore, from the reconstructed results, a threshold (=10%*maximum source density) was used to shrink the permissible region and reduce the number of unknown variables. The same reconstruction procedure was repeated. The reconstructed results correctly recovered the light source position and its power, which is in agreement with the truth with 1.5mm error in center location and 25% error in total power, as shown in Fig. 4 (a)-4(c).

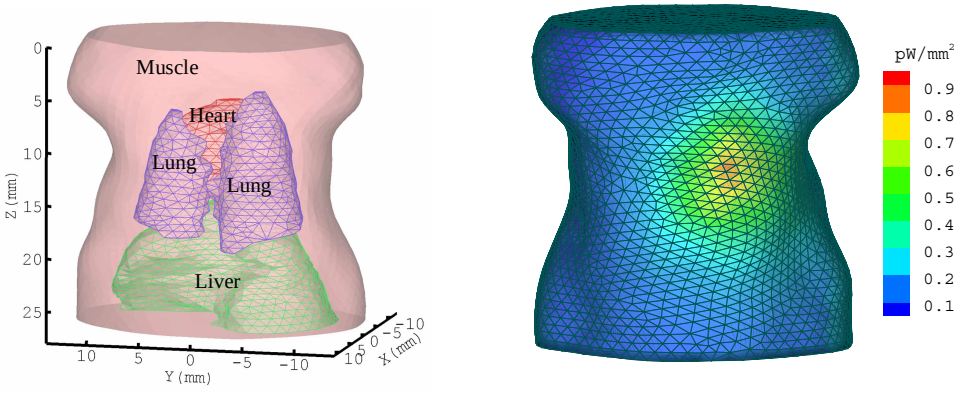

(a) (b)

Fig. 3. First mouse model and associated bioluminescent measurement. (a) A geometrical model of the mouse chest consisting of muscle, a heart, a lung and a liver, and (b) measured bioluminescent data mapped onto the finite element mesh model of the mouse chest.

Furthermore, we performed multiple reconstructions with different optical parameters to assess the sensitivity of our methodology to the variation of the optical properties. First, we conducted reconstructions based on 5% random variation of the optical parameters. In this case, the reconstructed results remained being good approximations to the true source. The average difference in the reconstructed light source position was about 0.85mm, and the average error in the estimated source power was about 20%. However, the larger the variation of the optical properties becomes, the poorer the BLT reconstruction quality would be. For example, in the cases of 20% variation of the optical parameters major discrepancies were observed in the BLT reconstruction. The differences in the reconstructed light source position were over 3mm, and the errors in the estimated source power were over 100%. All these data suggest that it is critically important to estimate *in vivo* optical properties as accurately as possible, preferably using a multi-spectral diffuse optical tomography (DOT) technique.

Additionally, we performed a BLT reconstruction based on an incorrectly assumed homogeneous mouse body geometrically identical to this mouse. The optical parameters of the homogeneous mouse were set to the corresponding means of the real values for all of the anatomical components. As we expected, the resultant reconstruction quality was seriously compromised, yielding the errors 3.53mm and 200% in terms of the source center and the source power, respectively

#70324 - $15.00 USD Received 26 April 2006; revised 27 July 2006; accepted 27 July 2006

Table 1. Optical parameters for the mouse organ regions

Material	Muscle	Lung	Heart	Liver	Kidney	Stomach
μ_a [mm^{-1}]	0.23	0.35	0.11	0.45	0.12	0.21
μ_s' [mm^{-1}]	1.00	2.30	1.10	2.00	1.20	1.70

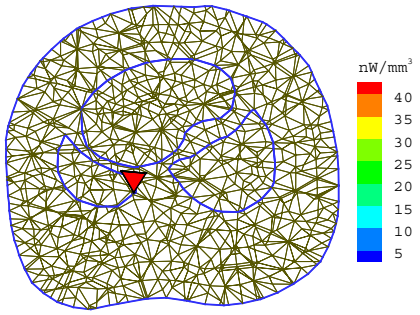

(a)

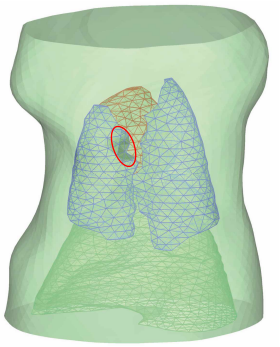

(c)

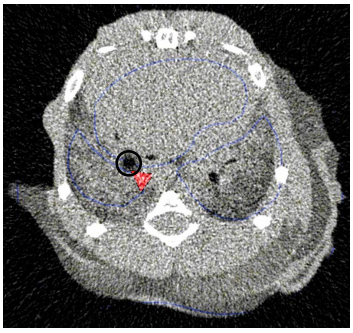

(b)

Fig. 4. BLT reconstruction of the luminescent source distribution in the first mouse. (a) A 2D transverse section of the reconstructed light source (red) and contours representing boundaries of various organs (blue), (b) the true source (inside the black circle) in a micro-CT slice superimposed with the reconstructed source (red) (the enlarged bronchus airway on the left is due to the inserted luminescent tube), and (c) a 3D rendering of the reconstructed source distribution (inside the red ellipse) in the mouse.

After the above technical validation of our BLT method, a tumor-bearing mouse was studied to demonstrate the biological feasibility of the BLT technology. In the mouse studies, we injected the 22Rv1-luciferase human prostate cancer cell line intracardially into scid mice as a xenograft model of prostate cancer metastasis [19]. The prostate cancer cells expressing firefly luciferase were introduced into the mice using the intracardiac injection technique. After several weeks, focal tumor growth was noted in a variety of sites such as bone, liver and adrenal gland. In each imaging experiment, a mouse was anesthetized with i.p. injection of 2.5% avertin 100μl/10g body weight, and injected with D-luciferin 100μl/10g body weight. The luciferase enzyme was combined with the substrate luciferin, Oxygen and ATP to generate bioluminescent photons in the mouse. Then, the mouse was similarly scanned using our BLT system, as shown in Fig. 5. We applied the same methodology to establish the geometrical model of the mouse with 87513 tetrahedral elements, 15971 nodes and 2912 detectors located on the side surface of the mouse. The optical parameters in Table 1 were assigned to the anatomical components. Then, the BLT reconstruction was done to localize and quantify the tumor cells in the mouse. The reconstructed source distribution was shown in Fig. 6(a), in which the stronger source has a power of 39.8nano Watts (right), and the smaller one has a power of 1.5nano Watts (left). After bioluminescence imaging experiment of the mouse, the mouse was dissected to find the tumors. As a result, two tumors were found on both adrenal glands, respectively, as shown in Fig. 6(b). The volume of tumor tissues as measured by Vernier calipers was 468mm^3 for the tumor on the right 275mm^3 for the tumor

#70324 - $15.00 USD Received 26 April 2006; revised 27 July 2006; accepted 27 July 2006

on the left. Thus, there was a considerable discrepancy between the relative difference between the power measurements (26.5-fold) and tumor volumes (1.7-fold). One possibility that will be examined in future studies is whether the power values are better correlated with viable tumor tissue rather than tumor volume, since tumor volume is a composite measurement of viable tumor cells (bioluminescent) and nonviable tumor cells as well as other components which are not bioluminescent. This has been suggested by previous studies [20]. Measurement of viable tumor cells *in vivo* using BLT may represent a better method for monitoring response to therapy than those methods that measure volume of tumor tissue such as MRI. The reconstruction took 180 seconds CPU time on a 3.2GHz Pentium 4 PC with 2GB memory.

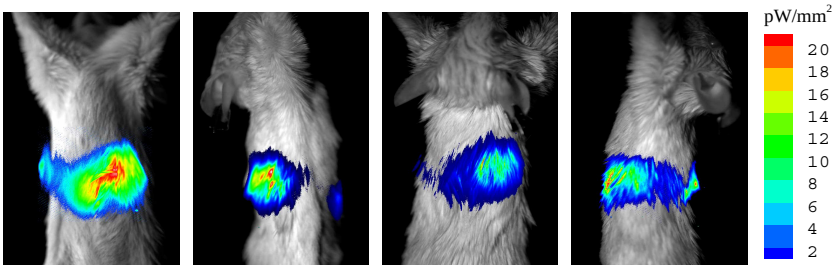

Fig. 5. Four bioluminescent views in pseudo-color superimposed on the corresponding photographs of the second mouse. (a)-(d) Anterior-posterior, right lateral, posterior-anterior and left lateral views, respectively.

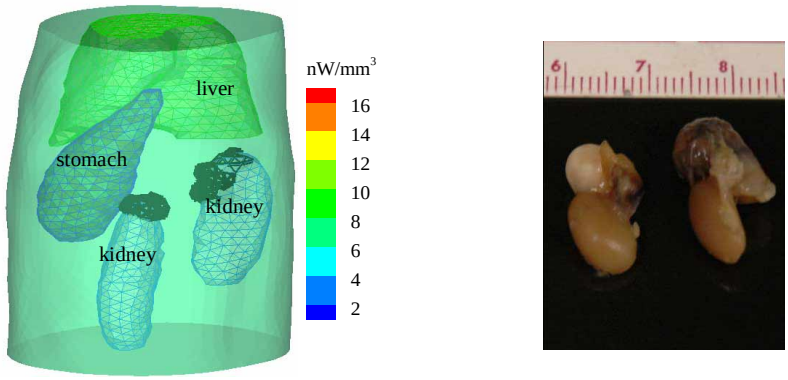

Fig. 6. BLT reconstruction and histological verification. (a) Two bioluminescent sources reconstructed on the two kidneys respectively, and (b) two tumors at the same locations on the dissected kidneys.

4. Discussion and conclusion

We have conducted *in vivo* mouse studies with BLT. Despite that BLT is not a well-posed problem in the general sense, it has been proven that the satisfactory solution can be obtained under practical constraints as *a priori* knowledge [6]. In our reconstruction process, the permissible source region has played an important role to enhance the numerical stability and computational efficiency.

We underline that the co-registration between synergic modalities is critical. The bioluminescent data on the body surface of a mouse not only depends on the light source

#70324 - $15.00 USD Received 26 April 2006; revised 27 July 2006; accepted 27 July 2006

distribution but also the anatomy and its optical properties. In the experiments, it is essential to keep the same posture of the mouse in the whole process. While it is impractical to describe every detail of the mouse anatomy, our atlas-based approach provides a practical geometrical model of the mouse.

Although the optical parameters of the organs and tissues are available in the literature, they are subject to substantial errors. The reconstruction results would be further improved with more accurate optical parameters and less measurement noise. An attractive way is to determine the optical parameters based on the mouse geometrical model using diffuse optical tomography. This approach may compensate for the anatomical complexity directly and establish the photon propagation model in the mouse optimally.

In summary, we have developed a BLT prototype and a rigorous methodology that compensates for the anatomical heterogeneity in the BLT image reconstruction, and demonstrated the validity of our technology and its feasibility in living mouse studies. Our results show that BLT can effectively localize and quantify the bioluminescent source inside a mouse, and may have a significant and lasting impact on the development of molecular medicine.

Acknowledgments

This work was supported by NIH/NIBIB EB001685. The authors thank the reviewers for their constructive comments.

#70324 - $15.00 USD Received 26 April 2006; revised 27 July 2006; accepted 27 July 2006